# Stochastic Model of a Liquid and Cold Neutron Scattering. II*

A. RAHMAN,† K. S. SINGWI, AND A. SJÖLANDER‡
*Argonne National Laboratory, Argonne, Illinois*
(Received September 13, 1961)

A simple model for the atomic motions in a liquid has been constructed based on the assumption that rapidly varying motions behave similarly to those in a solid, whereas slowly varying motions behave according to Langevin's equation for diffusion. This has been accomplished by writing the displacement of an atom as a sum of statistically independent "modes." Each "mode" is assumed to obey Langevin's equation for a harmonic oscillator with a certain frequency and a certain damping. To account for diffusion it is assumed that for "modes" below a certain frequency the harmonic restoring force is absent and thus these "modes" obey Langevin's equation for diffusion.

Based on this model, Van Hove's $G_s(\mathbf{r},t)$ function is Gaussian and its width function has been calculated. The computed scattering cross section for neutrons has been compared with experimental data for water and for liquid lead.

## I. INTRODUCTION

IN the preceding paper, hereafter referred to as I, the general theory of the scattering of slow neutrons by an interacting system was discussed. It was shown there that incoherent scattering could rigorously be discussed in terms of the velocity correlation functions of an atom in the system. More specifically, when a Gaussian approximation is made for the Van Hove $G_s(\mathbf{r},t)$ function, only the correlation function $\langle \mathbf{v}(0)\cdot\mathbf{v}(t)\rangle_T$ is required to evaluate the width function $\rho(t)$ but in the case of a liquid, it has not been possible to compute even this simple velocity correlation function from first principles. The formalism of paper I is, however, general enough to give some guidance in the construction of the width function $\rho(t)$. To make any further progress, one is obliged at this stage to take recourse to specific dynamic models of a liquid and subject them to experimental test.

The model that we shall discuss here is based on the conception that the heat motion of the atoms in a liquid is very similar to that in a solid. It is, of course, understood that proper account will have to be taken of the damping of the vibrations and of the self-diffusive motion of an atom in a liquid. This conception is not new, but has indeed been advocated by Frenkel[1] many years ago. More recently such ideas have been revived by Singwi and Sjölander[2] and by Rahman *et al.*[3] in their attempt to explain the observed energy spectra of neutrons scattered from a liquid.

Larsson and Dahlborg[4] have very recently studied in detail the scattering of cold neutrons from water and ice, and they find that there exists a great similarity in the scattered neutron spectra from these two substances so much so that these authors are lead to conclude that a quasi-crystalline model of water corresponds to physical reality.

The two characteristic features of these spectra are: (i) A narrow "quasi-elastic" peak, in fact much narrower than what we would expect on a simple diffusive model of a liquid; and (ii) an inelastic region devoid of almost any structure. The narrow "quasi-elastic" peak is an indication of the fact that an atom in a liquid is constrained to remain in its locality for a time period which is much greater than its "period of vibration." The inelastic scattering, analogous to that in a solid, is a manifestation of the development of the thermal cloud of an atom in a time period which is considerably smaller than the sedentary lifetime of the atom. The observed lack of structure in the inelastic region, in contrast to what one has in a solid, indicates that the vibratory motion of an atom in a liquid is highly damped.

## II. MODEL

In this model, we shall assume that the displacement of an atom in a liquid can be considered as a superposition of statistically independent components $\xi_s$, each of which obeys a Langevin-type equation of motion:

$$(d^2\xi_s/dt^2)+\beta_s(d\xi_s/dt)+\omega_s^2\xi_s=F_s(t), \qquad (1)$$

where $\beta_s$ is the damping constant and $F_s(t)$ is the stochastic force for the mode $s$. In writing Eq. (1), it is tacitly assumed that the effect of anharmonicity can be replaced by a stochastic force $F_s(t)$ and a damping force $\beta_s\dot{\xi}_s$, which is, indeed, the case if the anharmonic forces are small and can be treated by perturbation methods.[5] Obviously, such an equation would not lead to any diffusion since the mean position of each oscillator is never displaced. For the purpose of building into this picture a mechanism for diffusion, we remark the fact that the low frequency transverse modes cannot propagate in a liquid and should necessarily degenerate into a diffusive type of motion. This, however, is not the case

* Based on work performed under the auspices of the U. S. Atomic Energy Commission.
† On leave of absence from the Tata Institute of Fundamental Research, Bombay, India.
‡ Present address: University of Uppsala, Uppsala, Sweden.
[1] J. Frenkel, *Kinetic Theory of Liquids* (Oxford University Press, New York, 1946).
[2] K. S. Singwi and A. Sjölander, Phys. Rev. **119**, 863 (1961).
[3] A. Rahman, K. S. Singwi, and A. Sjölander, Phys. Rev., **122**, 9 (1961).
[4] K. E. Larsson and U. Dahlborg (unpublished).
[5] P. Mazur, Physica **25**, 149 (1959).

for longitudinal modes. As an approximation, one can assume that all "vibrations", including longitudinal, below a certain frequency $\omega'$ have no restoring force appearing in Eq. (1). For $\omega_s<\omega'$, Eq. (1), therefore, reduces to

$$(d^2\xi_s/dt^2)+\beta_s(d\xi_s/dt)=F_s(t). \quad (2)$$

This equation we know will give us a diffusive type of motion which we wish to incorporate in the model. We shall see later that to get agreement with experiments, the number of modes giving rise to diffusion has to be taken very small compared to the total number of modes.

As regards the spectrum of frequencies $\phi(\omega_s)$, the simplest approach is to consider it as the Debye type with a certain upper limit $\omega_D$ which gives the correct number for the degrees of freedom in the system. We have thus introduced two parameters, $\omega'$ and $\omega_D$, in the model. In the limiting case of a solid, we should have $\omega'=0$ and $\omega_D=k\theta_D/\hbar$, $\theta_D$ being the Debye temperature. As regards $\beta_s$ for the diffusive modes, we shall put it equal to a constant $\beta$ and for a vibrating mode, we shall take $\beta_s$ to be proportional to $\omega_s$. The latter assumption is based on the fact that in a solid the damping of the high frequency modes is approximately proportional to their frequency.[6] We thus have in the model two more parameters, $\beta$ and a constant of proportionality $\gamma$, which we shall refer to as the damping parameter. As we shall see, the diffusion constant $D$ can be written in terms of $\beta$, $\omega'$ and $\omega_D$. Hence, effectively, we have three parameters in this model which are at our disposal.

We can already see how these parameters will participate in producing the diffusion constant $D$. In the absence of all vibratory motions, we have $\omega'=\omega_D$ and we then know that $D=kT/M\beta$, $M$ being the mass of the atom and $T$ the temperature of the system.

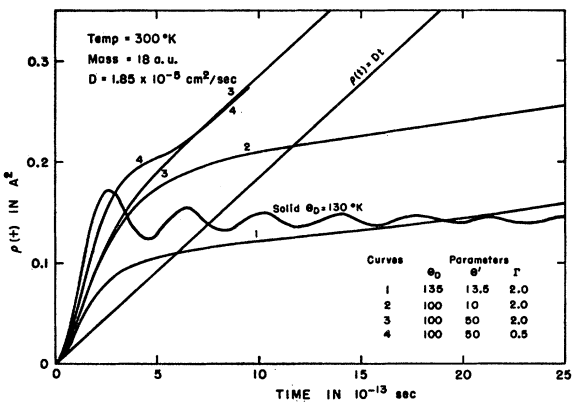


FIG. 1. Width function $\rho(t)$ for water for some values of the parameters; $\rho(t)$ for a solid ($\theta_D=130$°K) and that obtained from the diffusion equation is also shown.

[6] See K. F. Herzfeld and T. A. Litovitz, *Absorption and Dispersion of Ultrasonic Waves* (Academic Press Inc., New York, 1959).

With $(\omega'/\omega_D)^3$ modes participating in diffusion, we shall see that $D$ is given by $(\omega'/\omega_D)^3(kT/M\beta)$. In this model, therefore, the value of $\beta$ is smaller than the value $kT/MD$. We shall see that this circumstance will lead to a delay in the setting in of the diffusive behavior of the atom in a liquid.

To make use of Eq. (1), we assume further that the equilibrium distribution function for each velocity $\dot{\xi}_s$ is a Maxwellian distribution with a temperature $T$, common to all modes. This implies that the thermal average $\langle\dot{\xi}_s^2\rangle$ is equal to $kT/M$.

## III. MATHEMATICAL FORMULAS

The solution of the stochastic Eq. (1) has been discussed in detail by Chandrasekhar[7] and by Wang and Uhlenbeck.[8] Following Wang and Uhlenbeck we have

$$\langle\dot{\xi}_s(0)\dot{\xi}_s(t)\rangle_T=(kT/M)\exp(-\tfrac{1}{2}\beta_s t)\times\{\cos\omega_1 t-(\beta_s/2\omega_1)\sin\omega_1 t\}, \quad (3)$$

where

$$\omega_1=(\omega_s^2-\tfrac{1}{4}\beta_s^2)^{\frac{1}{2}}. \quad (4)$$

To get the velocity correlation $\langle\mathbf{v}(0)\cdot\mathbf{v}(t)\rangle_T$ we have to integrate (3) over the frequency spectrum $\phi(\omega_s)$, which is normalized such that $\int_0^\infty\phi(\omega_s)d\omega_s=1$. Using the fact that $\beta_s=\beta$ for $0\leqslant\omega_s<\omega'$ and $\frac{1}{2}\beta_s=\gamma\omega_s=\Gamma\omega_1$ for $\omega'\leqslant\omega_s\leqslant\omega_D$, we have

$$\begin{aligned}\langle\mathbf{v}(0)\cdot\mathbf{v}(t)\rangle_T&=3\langle v_x(0)v_x(t)\rangle_T\\&=3\int\phi(\omega_s)\langle\dot{\xi}_s(0)\dot{\xi}_s(t)\rangle d\omega_s\\&=\frac{3kT}{M}\left\{\left(\frac{\omega'}{\omega_D}\right)^3 e^{-\beta t}+\frac{3}{\omega_D{}^3}\int_{\omega'}^{\omega_D}d\omega_s\omega_s{}^2e^{-\Gamma\omega_1 t}\times(\cos\omega_1 t-\Gamma\sin\omega_1 t)\right\},\end{aligned} \quad (5)$$

where

$$1+\Gamma^2=(1-\gamma^2)^{-1}. \quad (6)$$

In the absence of damping, $\Gamma=0$.

Now $\rho(t)$ is given by [see Eq. (81) of paper I][9]

$$\rho(t)=(\hbar^2/8MkT)+\tfrac{1}{3}\int_0^t(t-t_1)\langle\mathbf{v}(0)\cdot\mathbf{v}(t_1)\rangle_T dt_1. \quad (7)$$

The term $\hbar^2/8MkT$ is insignificant here and will be neglected. Using (5) and (7), and performing the integration we have

[7] S. Chandrasekhar, Revs. Modern Phys. **15**, 1 (1943).

[8] M. C. Wang and G. E. Uhlenbeck, Revs. Modern Phys., **17**, 323 (1945).

[9] In Eq. (2) of reference 3, a factor $\frac{2}{3}$ before the integral sign has been missed in print. Also the definition of $\rho(t)$ here and in I differs from that in reference 3 by a factor two.

$$\rho(t)=\frac{kT}{M}\left\{\left(\frac{\omega'}{\omega_D}\right)^3\frac{e^{-\beta t}-1+\beta t}{\beta^2}+\frac{3}{\omega_D{}^3}[\Phi(\omega_D,t)-\Phi(\omega',t)]\right\}, \quad (8)$$

where

$$\Phi(\omega,t)=\omega-\frac{1}{t(1+\Gamma^2)^{\frac{1}{2}}}\exp\left(\frac{-\Gamma\omega t}{(1+\Gamma^2)^{\frac{1}{2}}}\right)\times\left\{(1-\Gamma^2)\sin\left(\frac{\omega t}{(1+\Gamma^2)^{\frac{1}{2}}}\right)-2\Gamma\cos\left(\frac{\omega t}{(1+\Gamma^2)^{\frac{1}{2}}}\right)\right\}. \quad (9)$$

It is easy to see that the expression for $\rho(t)$ has the correct form in the two limiting cases: (i) of a Debye solid at a temperature $T\gg\theta_D$ and (ii) of an atom diffusing according to Langevin's equation. For case (i) $\omega'=0$, $\Gamma=0$ and we have

$$\rho(t)=\frac{3kT}{M\omega_D{}^2}\left(1-\frac{\sin\omega_D t}{\omega_D t}\right), \quad (10)$$

and for case (ii) $\omega'=\omega_D$ and we have

$$\rho(t)=\frac{kT}{M}\frac{e^{-\beta t}-1+\beta t}{\beta^2}. \quad (11)$$

From Eq. (8), as can be verified easily, one gets the correct asymptotic diffusive form of $\rho(t)$, i.e., $Dt+C$, where $D$ is the diffusion constant. We get

$$D=(kT/M\beta)(\omega'/\omega_D)^3, \quad (12)$$

$$C=(3kT/M\omega_D{}^2)(1-\omega'/\omega_D)-D/\beta. \quad (13)$$

The fact that $(\omega'/\omega_D)$ as well as $\beta$ occur in Eq. (12) which gives $D$ is the significant difference from the simple Langevin's case where the parameter $\beta$ is determined uniquely by $D$. Due to the second term in (13), it is clear that $C$ can be made as large a negative constant as we like depending on the value of $\omega'/\omega_D$. A large negative value of $C$ corresponds to delayed diffusion. The width of the "quasi-elastic" peak in the scattered spectrum is controlled by this constant $C$; the larger the absolute value of $C$, the sharper is the peak. The parameter $\omega_D$ determines the size of the thermal cloud before diffusion becomes dominant, and the parameter $\Gamma$ determines the damping of the oscillations. As remarked in the introduction, there are only three arbitrary parameters in the present model.

## IV. RESULTS AND DISCUSSION

### Scattering in Water

In Fig. 1, we have given a whole series of curves for the width function $\rho(t)$, computed using Eq. (8), which clearly illustrate the influence of various parameters. $M$ has been taken equal to 18 atomic units (a.u.) since only the translational motion has been considered. The parameters $\omega'$ and $\omega_D$ are expressed as temperatures $\theta'$ and $\theta_D$ through the relation $\hbar\omega=k\theta$. It will be noticed that in curves 1 and 2, the asymptotic behavior of $\rho(t)$ is not yet apparent. However, the large value of the damping parameter prevents any wiggles in $\rho(t)$ which are so characteristic of a solid. The characteristic feature of curves 1 and 2 is thus a thermal cloud, which after a rapid initial rise, develops almost linearly for a considerable length of time, but with a very small slope. This rate of increase of the width of the thermal cloud is much smaller than the macroscopic diffusion constant $D$ which manifests itself after a much longer time period. In contrast to curves 1 and 2, curves 3 and 4 attain the asymptotic limit $Dt$ much more quickly. Curve 4 differs from curve 3 in having a smaller value of $\Gamma$ and that is why it is a little more wiggly, and this leads to a structure in the scattered spectrum.

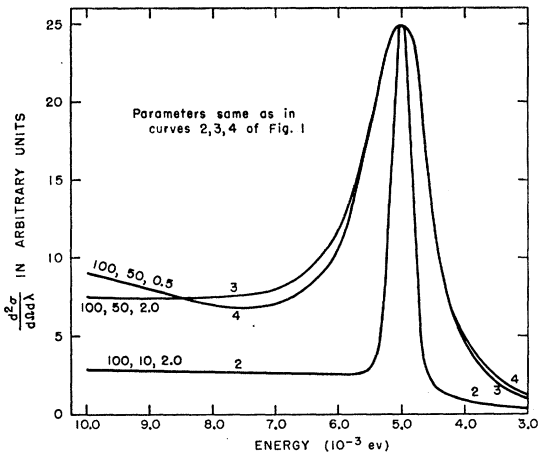


FIG. 2. Differential scattering cross section versus outgoing neutron energy for neutrons of incident energy $5.0\times10^{-3}$ ev scattered at 90° by water at 300°K. The curves are normalized in such a way that the maximum heights of the "quasi-elastic" peaks are the same in all cases.

In Fig. 2 is shown the differential scattering cross section calculated with some of the curves of Fig. 1, for an incident neutron energy of $5\times10^{-3}$ ev. The two characteristic features of all the curves of Fig. 2 are: (i) a narrow "quasi-elastic" peak and (ii) an inelastic part which is almost flat. Both these characteristics are consistent with observation. It will be noted that the sharpness of the "quasi-elastic" peak is a function of the quickness with which diffusion sets in. The part of curve 4 corresponding to inelastic scattering seems to show a very broad peak (not seen in Fig. 2), which is reminiscent of the one-phonon peak in a solid, in contrast to the case of curve 3 and this is because of a slightly wiggly nature of $\rho(t)$ in curve 4 of Fig. 1. The widths of the "quasi-elastic" peaks of curves 3 and 4, however, are the same since $\theta'/\theta_D$ for both curves is the same.

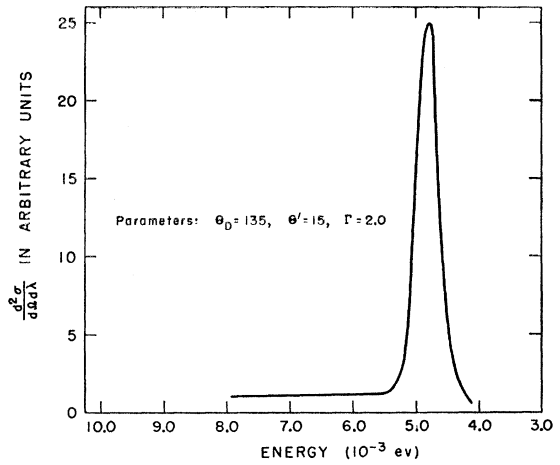


FIG. 3. Differential scattering cross section versus outgoing neutron energy for neutrons of incident energy $5.2\times10^{-3}$ ev scattered at 90° by water at 300°K, using parameters which gave the best fit to the experimental data of Larsson and Dahlborg[4] for beryllium-filtered neutrons.

Figure 3 shows the scattering for a monochromatic incident beam, and it should be compared with the scattered spectrum shown in Fig. 4, where the incident spectrum is taken to be $EdE$ with a sharp cutoff at $5.2\times10^{-3}$ ev (corresponding to the beryllium-filtered spectrum). The lack of any similarity between the two is quite remarkable, and it shows the difficulty in making any precise interpretation of the scattering data obtained with a filtered beam technique. Other aspects of the curves in Fig. 4 are self explanatory. The rise in the experimental curve in the energy range greater than $20\times10^{-3}$ ev is due to the contribution from the hindered rotations of the water molecules. The present model ignores the contributions of these rotations and is concerned only with hindered translations. It might be mentioned here that earlier Singwi and Sjölander[2] had calculated the inelastic scattering of beryllium-filtered neutrons in water, assuming it to be a solid with $\theta_D=135$°K and found a good fit between their computed curve and the experimental curve of

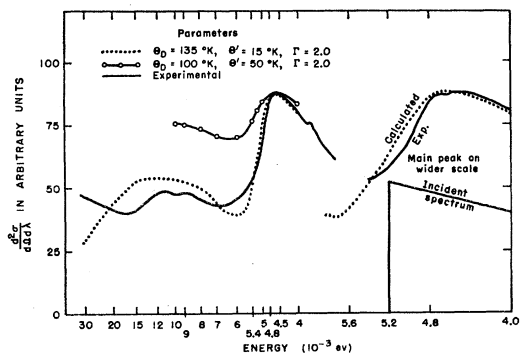


FIG. 4. Differential scattering cross section versus outgoing neutron energy for beryllium-filtered neutrons scattered at 90° by water at 300°K. The experimental curve is that of Larsson and Dahlborg.[4]

Hughes *et al.*[10] This good fit, as we have discovered it now, was the result of a mistake in the normalization, which if done correctly does not give an agreement.

We have not presented the calculated and observed spectra at a smaller scattering angle because it shows no new features. The fit is less satisfactory at 30° scattering angle.

In Fig. 5, the width of the "quasi-elastic" scattering is plotted as a function of the scattering angle for two sets of parameters. In the same figure is also given the width which one would expect on a simple diffusive model. The experimental points of Larsson and Dahlborg[4] are also shown. It will be seen that in the region of $\kappa$ values shown, no flattening out of the theoretical curves is apparent. This is in contrast with the results obtained by Singwi and Sjölander[2] on the basis of a model in which the width was primarily determined

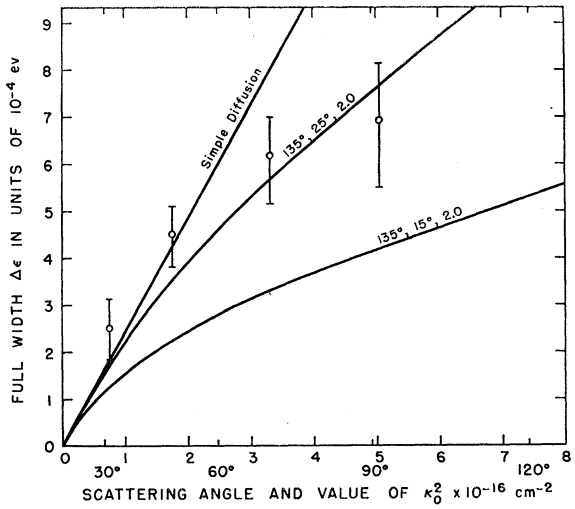


FIG. 5. Full width of the "quasi-elastic" peak versus $\kappa^2$ and the scattering angle, with $D=1.85\times10^{-5}$ cm$^2$/sec and $T=300$°K. Experimental results of Larsson and Dahlborg[4] are shown as circles.

through a decay factor of the type $e^{-t/\tau_0}$ and hence was independent of the scattering angle. Because of the large statistical uncertainties, it is hard to conclude from the experimental points if there is a genuine flattening of the curves for large scattering angles. It would be very desirable to measure the width as a function of the scattering angle more accurately than has hitherto been done. In the Appendix, we have constructed a very simple non-Gaussian model which gives for the width essentially the same result as obtained earlier by Singwi and Sjölander.[2] An important question which arises in this connection is whether the saturation of the width for large values of $\kappa$ is the result of a non-Gaussian $G_s(\mathbf{r},t)$, and whether this fact could be used to decide if $G_s(\mathbf{r},t)$ is Gaussian or non-Gaussian.

[10] D. J. Hughes, H. Palevsky, W. Kley, and E. Tunkelo, Phys. Rev. Letters **3**, 91 (1959).

One difficulty, however, is that for very large values of $\kappa$ there is no clear separation of the "quasi-elastic" scattering from the inelastic scattering and then the width in the above sense has no meaning.

From the numerical computation of the Fourier-transform, we find that the major contribution to the "quasi-elastic" scattering arises from the values of $\rho(t)$ in the time region in which it is almost flat and slowly rising as shown in curves 1 and 2 of Fig. 1. This implies that in the present model, the angular dependence of the width is determined by an "effective" diffusion constant much smaller than the ordinary diffusion constant $D$. One could say that the neutron is never able to "see" the macroscopic diffusive behavior but only the motion over that time period for which $\rho(t)$ has the above-mentioned behavior. However, for a very small $\kappa$, a larger and larger time period is scanned by the neutron and the width is then determined more and more by the actual asymptotic behavior of the diffusive motion of the atom. This is the reason why all curves of Fig. 5 merge into one another for $\kappa \rightarrow 0$.

## Scattering in Liquid Lead

In the foregoing, we have compared the calculated differential scattering cross section, based on our model, with the observed values for water and found that for certain values of the parameters, the agreement between the two is satisfactory. One might argue that water being a very special liquid in the sense that there exist strong hydrogen bonds between water molecules, it is not very surprising that a quasi-crystalline model should work. It would, therefore, be interesting to compare the results of this model in the case of a simple liquid. Unfortunately, the only other liquid for which some experimental data are available is liquid lead. The data using an incident monochromatic beam are of

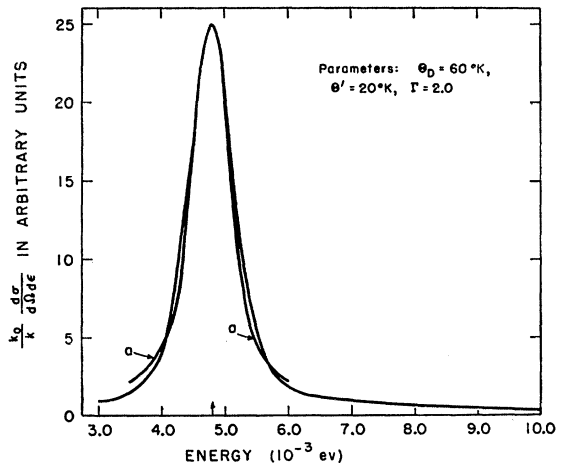


FIG. 6. Differential scattering cross section ($\times k_0/k$) versus outgoing neutron energy for neutrons of incident energy $4.8\times10^{-3}$ ev scattered at 90° by liquid lead at 620°K. Experimental curve of Brockhouse and Pope[12] is marked $a$.

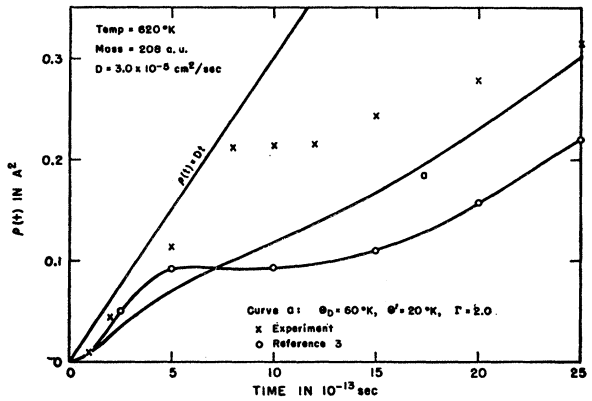


FIG. 7. Width function $\rho(t)$ for liquid lead for the same parameters as in Fig. 6. The width function used in reference 3 is shown by circles and that obtained by Brockhouse and Pope[12] from their experimental data is shown by crosses. The $\rho(t)$ obtained from the diffusion equation is also shown.

Turberfield[11] and of Brockhouse and Pope.[12] The former author has extended the observations into the inelastic region and has claimed a higher statistical accuracy, thus enabling him to measure the "quasi-elastic" and inelastic scattering simultaneously, whereas the latter authors used different incident energies to cover the inelastic region, and, therefore, they had to use normalization techniques to combine their observations.

In Fig. 6, we have plotted the scattering cross section as a function of the outgoing neutron energy for the values of the parameters shown. These values were chosen to fit the "quasi-elastic" scattering data of Brockhouse and Pope[12] shown as curve '$a$' in the figure. It will be seen that the agreement between theory and experiment is fairly good. Besides, the general shape of the curve in the inelastic region is in agreement with the observations of Turberfield[11]; in fact, the magnitude of the ratio of the elastic to the inelastic peak heights ($\approx 50$) is in agreement with his observations. While making this comparison, it must be clearly borne in mind that the calculations are based on the incoherent approximation.

In Fig. 7 is shown the width function $\rho(t)$ from which the scattering cross section of Fig. 6 was computed. For the sake of comparison, the values of the width function used in reference 3 by the authors have been shown as circles in Fig. 7. In the same figure is also shown the width function given by Brockhouse and Pope[12] who obtained it by double Fourier inversion of their observed scattering cross section. It will be seen that the two do not agree. The function $S(\kappa,\omega)$ (see paper I) which has to be subjected to the double Fourier transformation is to be constructed from the experimental data, and in constructing this function Brockhouse and Pope mention that they have made

[11] K. C. Turberfield (unpublished).

[12] B. N. Brockhouse and N. K. Pope, Phys. Rev. Letters 3, 259 (1959).

several approximations. It is difficult to say how their approximations affect the complicated mathematical transformation. Perhaps the reason for disagreement between the calculated curve and the "observed" values lies in this fact. To avoid all errors inherent in smoothing out the experimental observations, it may be better to compare the theoretical results directly with the observed scattering cross section.

## V. THE SPECTRUM OF THE VELOCITY CORRELATION FUNCTION

It has been shown in I that the Fourier transform, henceforth called the velocity spectrum, of the velocity correlation function $\langle \mathbf{v}(0)\cdot\mathbf{v}(t)\rangle_T$ can be used to express the width function $\rho(t)$ of the Gaussian $G_s(\mathbf{r},t)$ in a form which is formally identical with that for a harmonic solid. It was mentioned there that in the case of a harmonic solid this velocity spectrum is identical with the usual frequency spectrum of the normal modes. In the case of diffusive motions according to Langevin's equation, on the other hand, the velocity spectrum is easily seen to have a Lorentzian shape with a width $\beta=kT/MD$. The utility of the velocity spectrum in this context was first pointed out by Egelstaff *et al.*[13]

In this section, we shall discuss the velocity spectrum one obtains from the model under consideration. This will elucidate to some extent the physical meaning of the various parameters introduced in the model.

The normalized spectrum $f(\omega)$ was defined in Eq. (83) of I, and it was shown there [see Eq. (90)] that

$$f(\omega)=\frac{4M}{3\pi\hbar\omega}\tan h(\hbar\omega/2kT)\times\int_0^\infty \mathrm{Re}\langle \mathbf{v}(0)\cdot\mathbf{v}(t)\rangle_T\cos(\omega t)dt. \quad (14)$$

In the model the real part of $\langle \mathbf{v}(0)\cdot\mathbf{v}(t)\rangle_T$ is approximated by the corresponding classical correlation function. For consistency in the approximation we must also take $\tanh(\hbar\omega/2kT)=\hbar\omega/2kT$ and hence

$$f(\omega)=(2M/3\pi kT)\int_0^\infty \langle \mathbf{v}(0)\cdot\mathbf{v}(t)\rangle_{\mathrm{cl}}\cos(\omega t)dt. \quad (15)$$

Using Eq. (5) we get

$$f(\omega)=\frac{2}{\pi}\left\{\left(\frac{\omega'}{\omega_D}\right)^3\frac{\beta}{\beta^2+\omega^2}+\frac{3\gamma}{\omega_D}\left(\frac{\omega}{\omega_D}\right)^2\times\int_{\omega'^2}^{\omega_D^2}\frac{xdx}{(x-\omega^2)^2+4\gamma^2\omega^2x}\right\}. \quad (16)$$

It is easy to see that $f(0)=2MD/\pi kT$.

In Fig. 8 we have plotted $\omega_D f(\omega)$ for some of the values of the parameters $\omega'$, $\omega_D$, $\Gamma$, which were used in Fig. 1 to illustrate how they determine the shape of $\rho(t)$; the shape of $f(\omega)$ shows more strikingly the role played by each of the three parameters. Figure 9 shows the velocity spectrum for lead with the same parameters as in Fig. 6.

In the case of an undamped Debye solid, we have $\omega_D f(\omega)=3(\omega/\omega_D)^2$ whose maximum value is attained at $\omega=\omega_D$. With damping, however, this sharp cutoff goes over into a smooth curve with a tail, thus depressing the maximum height of the curve. As will be seen from Figs. 8 and 9, the maximum value of $\omega_D f(\omega)$ appears to be a function of the damping parameter only. The parameter $\omega_D$ determines the region in which $f(\omega)$ attains its maximum value.

When $\omega'/\omega_D$ is small, i.e., when the number, $(\omega'/\omega_D)^3$, of diffusive modes is small, we see that $f(\omega)\propto\omega^2$ down to frequencies in the neighborhood of $\omega'$, where it suddenly rises to give the value $2MD/\pi kT$ at $\omega=0$. This sharp rise is probably a consequence of the way diffusive modes have been introduced in our model, i.e., by assuming the diffusion Eq. (2) to hold for all frequencies $\omega_s<\omega'$.

It will be noticed from Eq. (16) that $f(\omega)$ goes to zero for large values of $\omega$ as $1/\omega^2$. This is a consequence of the non-analytic behavior of the velocity correlation function for $t=0$; both for the diffusive part and the vibratory part we have a term of the form $\exp(-c|t|)$. In an exact model, this is certainly not the case, and we would expect the exact velocity spectrum to decrease for $\omega\to\infty$ more rapidly than any power of $1/\omega$ (see Sec. VII in I).

In the case of water, it may seem questionable whether one should use the mass of the hydrogen atom or the mass of the water molecule when defining the frequency spectrum. From the discussion in I, it is clear that if one includes in $f(\omega)$ the effects of translational as well as rotational and vibrational motions of the water molecules, the mass of the hydrogen atom should appear in the definition of $f(\omega)$ [Eq. (89) of I]; consequently,

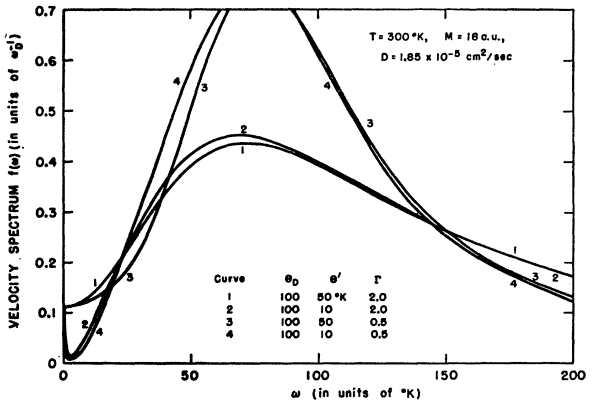


FIG. 8. The velocity spectrum for water for some values of the parameters.

[13] P. A. Egelstaff, S. J. Cocking, R. Royston, and I. M. Thorson, Proceedings of the Symposium on Slow Neutron Scattering, International Atomic Energy Agency, Vienna, 1960 (unpublished).

$f(0)=2M_HD/\pi kT$, as is also apparent from the experimentally determined $f(\omega)$ of Egelstaff *et al.*[13]

If, as in our model, only translational motion of the water molecules is considered the velocity correlation function should be that of the center-of-mass motion and the velocity spectrum will be a part of the complete one. If the rotational and vibrational motions contribute only to high-frequency components of the spectrum, the shape of the low-frequency part is determined by the translational motion only. Thus the velocity spectrum in our model will differ from the complete one by a factor $M_{H_2O}/M_H$ since the area under $f(\omega)$ has been normalized to unity. As regards $f(\omega)$ determined by Egelstaff *et al.*[13] it is not possible to compare their spectrum with ours due to the fact that their resolution covers almost the whole region of interest in Figs. 8 and 9.

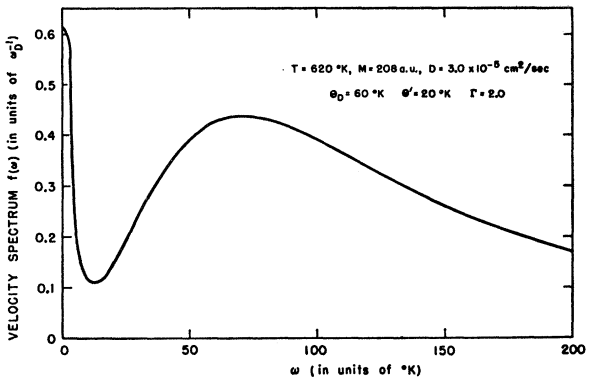


FIG. 9. The velocity spectrum for liquid lead for the same values of the parameters as in Figs. 6 and 7.

## VI. GENERAL REMARKS

We might mention here the reasons which led us to abandon our earlier model[3] in favor of the present one. The first and the most important reason was that with a given set of parameters, we found it impossible to fit simultaneously "quasi-elastic" and inelastic scattering regions. This was tried in the case of water for which experimental data were available. The theoretical $\rho(t)$ in the earlier model invariably exhibited a wiggly behavior, whereas the observed cross section is flat in the inelastic region. The reason for the wiggly nature of $\rho(t)$ in the earlier model is that all frequencies are damped equally, whereas in the present model the damping is proportional to the frequency of the "mode." The $\rho(t)$ curves (Fig. 1) in the present model are comparatively less wiggly. Secondly, the present model has a more physical basis behind it than the earlier one has. From the very nature of the model and from the smallness of the values of the ratio $\omega'/\omega_D$ required to fit the neutron data, it is obvious that the thermodynamic properties of a liquid such as the specific heat will be close to that of a solid at high temperature which in fact, is the case. In fact, for all physical phenomena involving a time scale less than a few times $10^{-12}$ sec, a liquid would behave like a solid. For example, it would exhibit rigidity under the influence of an external force if the time period of the force is less than the above relaxation time of the liquid. The conventional experimental techniques have so far failed to reveal this solid-like behavior of a liquid because of the very short relaxation time.

The value of the damping parameter $\Gamma$ used in our computation has reached a saturation value in the sense that any further increase of its value does not change $\rho(t)$. This means that there are, in fact only two adjustable parameters $\omega'$ and $\omega_D$ in the model. The value of $\Gamma$ used is 2.0, which results in the damping of the modes in a time period which is one-sixth the period of the mode. Under such circumstances, it is physically meaningless to talk of modes in the sense one does in a solid. In the present context, they have been introduced rather as a mathematical concept.

As regards the number of parameters which one should logically expect to be essential for the description of self-diffusion in liquids, firstly, one should have a diffusion constant and a constant to delay the diffusion or, equivalently, to specify the number of diffusive modes; secondly, the vibratory behavior before diffusion sets in requires a damping parameter and a frequency spectrum and the latter under the simplifying assumption of a Debye type spectrum requires a cutoff Debye frequency. This is probably the minimum number of parameters required for a physically admissible picture of self-diffusion in liquids.

## APPENDIX

After the initial development of the thermal cloud has taken place, we shall suppose that the intermediate scattering function $F_s(\kappa,t)$ is given by

$$F_s(\kappa,t)=e^{-\alpha|t|}\exp(-\kappa^2R^2)+(1-e^{-\alpha|t|})\exp[-\kappa^2\gamma(t)], \quad \text{(A1)}$$

where $R$ is a constant. This function is evidently the Fourier transform of a non-Gaussian $G_s(\mathbf{r},t)$ which is a sum of two functions each one of which is a Gaussian function. One of them has a width $[\gamma(t)]^{\frac{1}{2}}$ which is a function of time and the other has a constant width $R$. Physically, this corresponds to a model in which diffusion is pictured as an evaporation process from a probability cloud which has a certain size at time $t=0$. As time progresses, the probability density in the cloud diminishes, and the gradual development of its wings takes place in a Gaussian fashion. The spreading of the wings with time corresponds to diffusion.[14]

[14] This mechanism of diffusion in a liquid is similar to that in a solid with the difference that in a solid the probability density is anisotropic being large only at the lattice sites or at the interstitial positions $\Gamma$; whereas in a liquid the probability density is isotropic.

The "quasi-elastic" scattering is given by

$$\left(\frac{d^2\sigma}{d\Omega d\omega}\right)_{\text{qu-el}} = N\frac{a^2}{2\pi}\frac{k}{k_0}\int_{-\infty}^{\infty} e^{-i\omega t}F_s(\kappa,t)dt. \quad \text{(A2)}$$

Substituting for $F_s(\kappa,t)$ from (A1) into (A2) and performing the integration, we have

$$\left(\frac{d^2\sigma}{d\Omega d\omega}\right)_{\text{qu-el}} = N\frac{a^2}{\pi}\frac{k}{k_0}\left(e^{-2W}\frac{\alpha}{\alpha^2+\omega^2}+\frac{(\kappa^2D)}{(\kappa^2D)^2+\omega^2} - \frac{\alpha+\kappa^2D}{(\alpha+\kappa^2D)^2+\omega^2}\right), \quad \text{(A3)}$$

where we have put $\kappa^2R^2=2W$, the Debye-Waller factor. In deriving (A3) we have assumed that $\gamma(t)=D|t|$, $D$ being the diffusion constant.

Let us consider the following two cases:

Case (i), $\alpha\ll\kappa^2D$ or $\kappa^2D\tau_0\gg1$, where $\tau_0=1/\alpha$. In this case, (A3) simplifies to

$$\left(\frac{d^2\sigma}{d\Omega d\omega}\right)_{\text{qu-el}} = N\frac{a^2}{\pi}\frac{k}{k_0}e^{-2W}\frac{\tau_0}{1+\omega^2\tau_0^2}. \quad \text{(A4)}$$

The full width $\Delta\epsilon$ of the peak is $2\hbar/\tau_0$.

Case (ii), $\alpha\gg\kappa^2D$ or $\kappa^2D\tau_0\ll1$, and further, if $e^{-2W}\approx1$, (A3) simplifies to

$$\left(\frac{d^2\sigma}{d\Omega d\omega}\right)_{\text{qu-el}} = N\frac{a^2}{\pi}\frac{k}{k_0}\frac{\kappa^2D}{(\kappa^2D)^2+\omega^2}. \quad \text{(A5)}$$

The full width of the peak is $2\hbar\kappa^2D$. The results obtained here in a simple manner are essentially the same as those obtained earlier by Singwi and Sjölander[2] from more detailed considerations. Thus we see that in this non-Gaussian model we get a saturation effect for the width function for large values of $\kappa$ which is not the case, as we have seen before, in the Gaussian model.

PHYSICAL REVIEW VOLUME 126, NUMBER 3 MAY 1, 1962

# Hyperfine Structure of Praseodymium-142†

AMADO Y. CABEZAS,* INGVAR P. K. LINDGREN,‡ RICHARD MARRUS, AND WILLIAM A. NIERENBERG§
*Lawrence Radiation Laboratory and Department of Physics, University of California, Berkeley, California*

(Received December 21, 1961)

The hyperfine structure of 19-hr $Pr^{142}$ in the electronic ground state $^4I_{9/2}$ has been studied by the atomic-beam magnetic-resonance method. The following results have been obtained: electronic splitting factor $g_J(^4I_{9/2})=-0.7322(3)$, nuclear spin $I=2$, magnetic-dipole hyperfine-structure constant $|A|=67.5(5)$ Mc/sec, electric-quadrupole hyperfine-structure constant $|B|=7.0(2.0)$ Mc/sec, and $B/A>0$. From the hyperfine-structure constants, and assumptions made concerning the electronic fields at the nucleus, the nuclear moments are calculated to be $|\mu_I|=0.297(15)$ nm, and $|Q|=0.035(15)$ b, with $Q/\mu_I>0$.

## INTRODUCTION

PRECISION investigations of hyperfine structure by the method of atomic beams can yield information about the electronic structure of the low-lying atomic states, and the structure of the nuclear ground state. Some features of the electronic ground state of praseodymium (Pr) have already been established by the atomic-beam work of Lew.[1] In particular, this work showed that the ground configuration of Pr is $(4f)^3$, and that coupling among the electrons to the Hund's rule state $^4I_{9/2}$ gives good agreement with the measured electronic angular momentum ($J$) and electronic splitting factor ($g_J$). This coupling scheme seems to be characteristic of all the elements in the lanthanide series that contain $4f$ electrons only.[2] Corrections to the $g_J$ values of systems containing $4f$ electrons arise from the breakdown of Russell-Saunders coupling and relativistic and diamagnetic effects. These have been recently calculated[3] and have yielded, for Pr, the value $g_J=-0.7307$. As a check of this theory it seemed to us desirable to obtain a more accurate experimental value for the $g_J$ value than that given by Lew.

Praseodymium-142 has 59 protons and 83 neutrons, and, therefore, lies in the region of the table of isotopes that should be well described by the shell model. On the basis of the single-particle shell model, the ground-state properties are determined by the states of the last proton and neutron. The shell model predicts that the 59th proton should lie in the $d_{\frac{5}{2}}$ state. This is supported by the observed spin of $Pr^{141}$. The state of the 83rd neutron is very probably $f_{7/2}$, as inferred from the level-

† Work done under the auspices of the U. S. Atomic Energy Commission.

* Present address: Convair Astronautics, San Diego, California.
‡ Present address: Institute of Physics, University of Uppsala, Uppsala, Sweden.
§ Now on leave as Science Advisor to NATO.

[1] Hin Lew, Phys. Rev. **91**, 619 (1953).

[2] A. Cabezas, I. Lindgren, and R. Marrus, Phys. Rev. **122**, 1796 (1961).

[3] B. R. Judd and I. P. K. Lindgren, Phys. Rev. **122**, 1802 (1961).